

CMOS Integrated Microsystems and Nanosystems

Henry Baltes and Oliver Brand

Physical Electronics Laboratory, ETH Zurich
CH-8093 Zurich, Switzerland

ABSTRACT

We review selected micro- and nano-systems developed recently at the Physical Electronics Laboratory of ETH Zurich using industrial CMOS technology in combination with post-processing micromachining and film deposition: (i) an infrared sensor microsystem for presence detection of persons, (ii) calorimetric, capacitive, and gravimetric chemical sensor microsystems for detection of volatile organic compounds in air, and (iii) a parallel scanning AFM chip. The microsystems combine sensor structures and read-out circuitry on a single chip.

Keywords: CMOS, microsystem, nanosystem, infrared radiation sensor, chemical sensor, AFM

1. INTRODUCTION

Micro- and nanosystems based on CMOS IC technology became feasible when CMOS-compatible micromachining was established. Fabrication steps added to the regular CMOS process include, e.g., anisotropic etching of silicon or thin film deposition of “non-IC” materials. Preferably, these fabrication steps are performed as *post-processing* or *post-CMOS*, i.e., after completion of the regular IC process sequence. However, they can also precede the IC process (*pre-CMOS*) or can be performed in-between the regular IC steps (*intermediate processing*).

In the case of *post-processing*, the additional process steps have to be compatible with the foregoing IC process. Different post-CMOS fabrication processes used at the Physical Electronics Laboratory (PEL) of ETH Zurich, Switzerland, have been presented earlier [1,2], including an overview given at the 1998 *SPIE Smart Electronics & MEMS Symposium* [2].

In this paper, recent examples of post-CMOS micro- and nanosystems are presented:

- Infrared sensor microsystem for presence detection of persons
- Three different chemical microsystems for detection of volatile organic compounds in air
- CMOS AFM probe for parallel scanning atomic force microscopy

Further author information

H. Baltes, Email: baltes@iqe.phys.ethz.ch, Telephone: +41-1-633 2089, Fax: +41-1-633 1054, WWW: <http://iqe.ethz.ch/pel>

2. INFRARED SENSOR MICROSYSTEM

Thermoelectric infrared (IR) sensor microsystems are developed at the Physical Electronics Laboratory (PEL) for detection of the presence of persons by means of their emitted infrared radiation. The microsystems consist of either a pair or an array of infrared sensors cointegrated on a chip with dedicated signal conditioning circuitry [3]. Incoming infrared radiation is absorbed in the dielectric layer sandwich of the CMOS process [4] and heats up a thermally insulated sensor area, either a membrane or a beam structure. The temperature elevation is measured using an integrated thermopile and amplified using an on-chip amplifier.

The microsystems are fabricated using industrial CMOS processes in combination with post-processing micromachining to form the thermally insulated sensor structure consisting of a sandwich of the CMOS dielectric layers. While dielectric membranes are released using an anisotropic etching step from the back of the wafer, beam-type structures are released in a maskless etching step from the front of the wafer [1]. Polysilicon and aluminum lines sandwiched in-between the dielectric layers form either polysilicon/aluminum or n^+ -polysilicon/ p^+ -polysilicon thermopiles for temperature sensing [3].

Fig. 1 shows a CMOS infrared sensor microsystem mounted on a TO header [3]. It consists of two $700\ \mu\text{m}$ by $1500\ \mu\text{m}$ dielectric membranes carrying each a thermopile with 118 n^+ -polysilicon/ p^+ -polysilicon thermocouples. The membrane sensors have a sensitivity of $45.8\ \text{V/W}$ and a noise equivalent input power of $4.2\ \text{nW}$. The two thermopiles are connected in parallel to an on-chip differential low-noise amplifier utilizing the auto-zero technique in a switched capacitor implementation to suppress flicker noise [5]. The white noise spectrum was measured to be $317\ \text{nV/Hz}^{1/2}$ [3]. Additional circuit-blocks integrated on-chip include a low-pass filter, a bandgap-reference voltage generator, an oscillator and the output stage. The complete microsystems covers a chip area of approximately $3.5\ \text{mm}$ by $3\ \text{mm}$.

The microsystem was fabricated using a $2\ \mu\text{m}$ double-polysilicon, double-metal CMOS technology provided by EM Microelectronic-Marin SA, Switzerland. The membranes were released using a post-processing KOH etching step with the thermal oxide of the CMOS process as etch-stop layer [3].

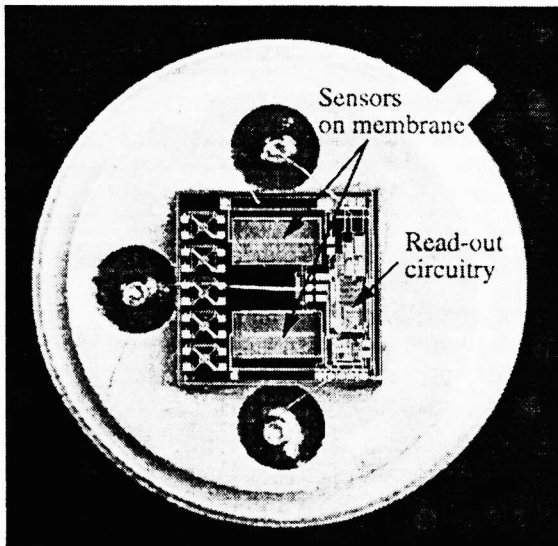


Fig. 1: Photograph of CMOS thermoelectric infrared sensor for presence detection mounted on a TO header; the CMOS chip includes two thermopiles, each located on a $700\ \mu\text{m}$ by $1500\ \mu\text{m}$ dielectric membrane, and signal conditioning circuits [3].

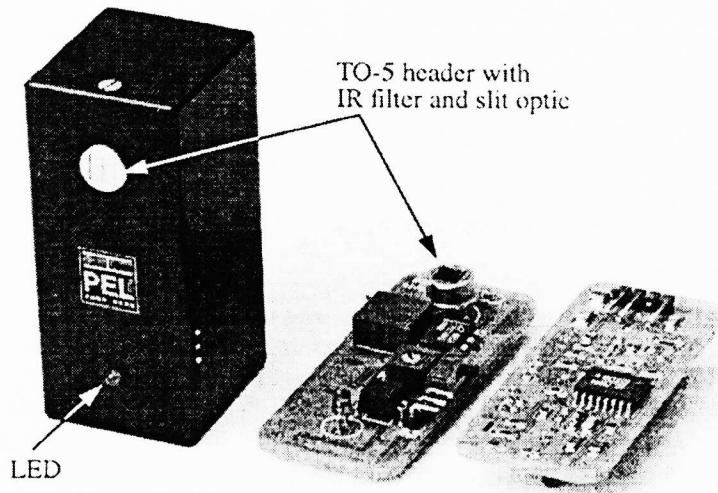


Fig. 2: Photograph of intrusion detector demonstrator; the printed circuit board contains the CMOS IR microsystem (see Fig. 1) in a TO header with infrared entrance filter and additional signal processing electronics [3]; the height of the housing is $62\ \text{mm}$.

Based on the microsystem shown in Fig. 1, a hand-held demonstrator system for presence detection has been built (see Fig. 2, [3]). To this end, the microsystem mounted in a TO-5 header is covered with a custom cap containing an IR filter window. A chrome layer on top of the window is structured to form a simple slit optic. Using this setup, the two sensor elements

receive infrared radiation from two separate space sectors. An infrared radiation source present in only one of the sectors is detected, while uniform background radiation present on both sectors is cancelled out by the differential sensor arrangement. The output signal of the CMOS infrared microsystem, namely the amplified difference of the two sensor signals, is further processed using external circuit components mounted on a common Printed-Circuit-Board (PCB). If the sensor output voltage exceeds a certain adjustable threshold, the detector indicates the presence of a person by switching on an LED. The demonstrator is able to detect the presence of a person at a distance of up to four meters [3].

Besides the presence detection systems, arrays of thermoelectric infrared sensors have been fabricated using CMOS technology for thermal imaging [1, 6].

3. CHEMICAL MICROSENSORS

The Physical Electronics Laboratory develops CMOS chemical microsensors for detection of volatile organic compounds (VOCs) in air. Chemical sensing is achieved by depositing chemically sensitive layers on physical sensor structures. Polymers films, such as polyurethane and polysiloxane derivatives, are used as chemically sensitive layers for monitoring the whole spectrum of organic volatiles in air. These polymers offer a compromise between selectivity towards certain analytes and reversibility of the polymer/analyte interaction. Moreover, the polymers are compatible with CMOS technology and can be applied using, e.g., spray-coating through a shadow mask. Upon absorption of analyte gas molecules, a physical property of the polymer, such as its mass, dielectric constant, or temperature, changes, which is monitored by the physical sensor structure. At PEL, three different sensing principles are currently investigated:

- Calorimetric chemical microsensors [7]
- Capacitive chemical microsensors [8]
- Gravimetric chemical microsensors [9]

The CMOS fabrication approach makes it possible to combine all three chemical sensor types together with their signal conditioning circuitry on a single chip. Arrays of sensors featuring different operation principles and different polymer films are used to improve the selectivity of the chemical microsystem. The goal is the development of a “micronose”, a small, inexpensive chemical sensor system for detection of VOCs in industrial and environmental applications, such as on-line process monitoring, personal safety, and threshold limit value (TLV) monitoring. An experimental “micronose” combining capacitive and resonant chemical sensors on a CMOS chip has been described recently [10].

Calorimetric Chemical Microsensor

The calorimetric chemical microsystem (see Fig. 3) uses a physical sensor structure similar to that of the infrared sensor described earlier to detect enthalpy changes during analyte absorption and desorption. It consists of two 700 μm by 1500 μm dielectric membranes in a differential arrangement, one covered with the chemically sensitive polymer and one uncovered reference [7]. Enthalpy changes during absorption and desorption of gaseous analytes into the polymer cause temperature variations of the polymer coated thermally insulated micromachined membrane. Polysilicon/aluminum thermopiles consisting of 44 thermocouples are sandwiched in-between the dielectric membrane layers to measure these temperature variations. The difference of the sensor and reference thermopile output voltage is amplified on-chip using a low-noise amplifier. The three-stage low-noise chopper stabilized instrumentation amplifier features a gain of 2500 and a bandwidth of 500 Hz with an equivalent input noise of $15 \text{ nV}/(\text{Hz})^{1/2}$ [11].

The calorimetric chemical microsystem is fabricated using a 1 μm single-poly, double-metal CMOS process of EM Micro-electronic-Marin SA, Switzerland. As in the case of the infrared sensors, the dielectric membranes with integrated thermopiles are released using an anisotropic KOH etching step from the rear of the wafer with an etch-stop at the thermal oxide of the CMOS process [7].

In contrast to the capacitive and gravimetric chemical sensors described in the following, the calorimetric microsystem measures transient signal, i.e., only changes in the analyte concentration result in an output signal. Therefore, the “air under test” is chopped with a reference gas in order to create the required transient input signals. At PEL, the chemical microsensors are tested in a computer controlled flow setup by switching between constant analyte concentrations and synthetic air as reference/carrier gas at a constant flow rate. Varying concentrations of different volatile organic compounds are generated by mix-

ing saturated vapors from thermostated bubblers with synthetic air through computer controlled mass flow controllers. For testing, the chemical microsensor dice are mounted in standard Dual-In-Line packages which are directly attached to the measurement chamber using a metal seal.

Figs. 5(a) and (b) show the signals obtained for switching on and off 4000 ppm of toluene, respectively. While the temperature of the sensing membrane increases upon analyte absorption into the polymer resulting in a positive signal peak, it decreases upon analyte desorption causing a negative signal peak. The shape of the output signal, i.e., the maximum signal

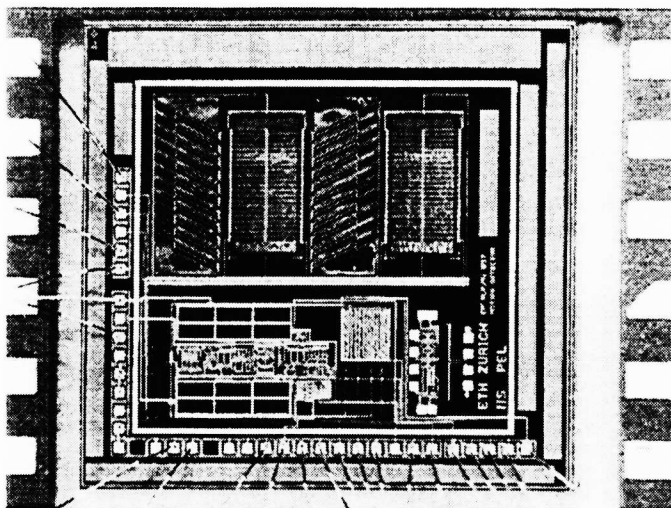


Fig. 3: Micrograph of CMOS chemical calorimetric sensor system consisting of polymer coated sensing membrane, uncoated reference membrane, and low-noise differential amplifier; the 700 μm by 1500 μm membranes are released in a post-CMOS anisotropic etching step using KOH [7].

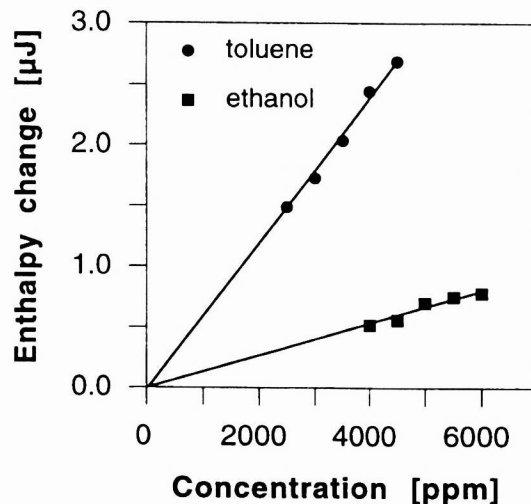


Fig. 4: Absolute values of measured enthalpy changes as a function of the analyte concentration at 200 sccm and 28 $^{\circ}\text{C}$ [7]; the different slopes for toluene and ethanol reflect differences in the saturation vapor pressure, heats of vaporization, and different affinity of the polymer towards the analyte.

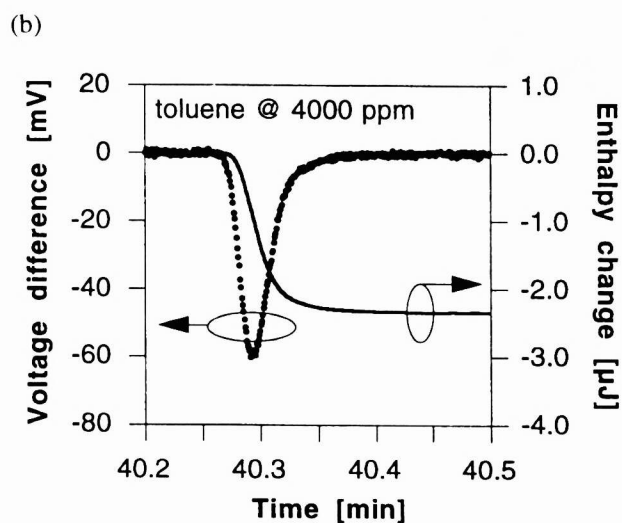
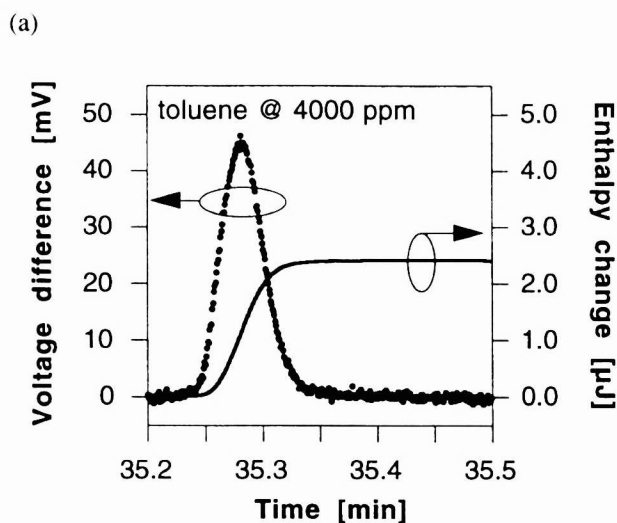


Fig. 5: Output signal of the calorimetric chemical microsystem while switching (a) on and (b) off 4000 ppm of toluene using a computer controlled flow setup at 200 sccm and 28 $^{\circ}\text{C}$ [7]; the resulting enthalpy change was calculated by integrating the sensor output signal and calibrating with the microsystem sensitivity $S = 51.1 \text{ mV}/\mu\text{W}$.

amplitude and the width of the signal peak, depend on the measurement setup and vary from absorption to desorption. In contrast, the resulting enthalpy change, i.e., the integral of the sensor output over time, is a characteristic for the analyte/polymer interaction and is the same for absorption and desorption. To obtain the enthalpy change, the sensor output voltages need to be calibrated. To this end, a polysilicon heating resistor is integrated on both the sensor and the reference membrane. Heating the membranes with known heating powers and measuring the amplified thermopile output voltages gives sensitivities of 51.1 mV/ μ W and 51.3 mV/ μ W for sensor and reference, respectively. Using these sensitivities the enthalpy changes due to analyte absorption/desorption can be calculated (see Fig. 5). The measured enthalpy changes as a function of the analyte concentration for toluene and ethanol are summarized in Fig. 4. The different slopes indicate the different sensitivities of the calorimetric microsystem towards these analytes.

Capacitive Chemical Microsystem

A capacitive chemical microsystem consisting of three polymer coated sensing capacitors, three uncoated reference capacitors, a multiplexer, and a $\Sigma\Delta$ -modulator for signal read-out is shown in Fig. 6 [8]. The microsystem is fabricated using a 0.8 μ m double-poly, double-metal CMOS process of Austria Mikro Systeme International (AMS), Austria. The interdigitated capacitor structures are formed by the metal layers of the CMOS process. The polymer coated sensing capacitance and the uncoated reference capacitance are incorporated in the first stage of a second order switched capacitor $\Sigma\Delta$ -modulator. The on-chip multiplexer is used to switch between the different sensing capacitors and references. To improve the selectivity of the chemical microsystems towards certain analytes, the array of sensing capacitors is coated with different polymer layers [8].

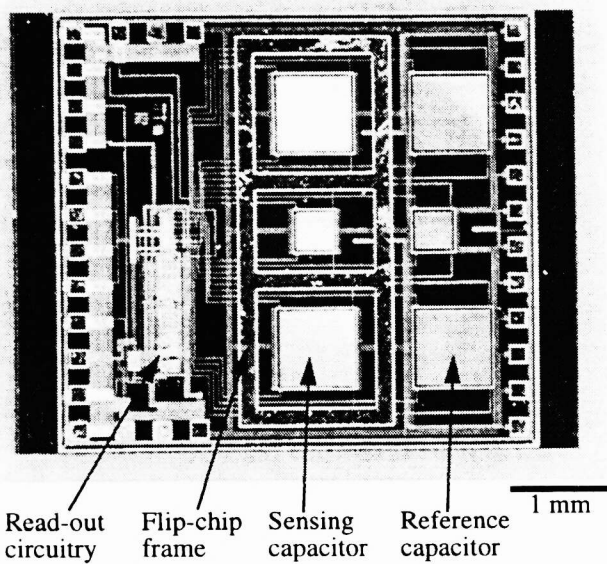


Fig. 6: Capacitive CMOS chemical microsystem consisting of three sensing capacitors, three reference capacitors, and read-out circuitry; the sensor was fabricated using a 0.8 μ m CMOS technology of AMS; the chemically sensitive polymer films are spray-coated onto the sensing capacitors after completion of the CMOS process [8].

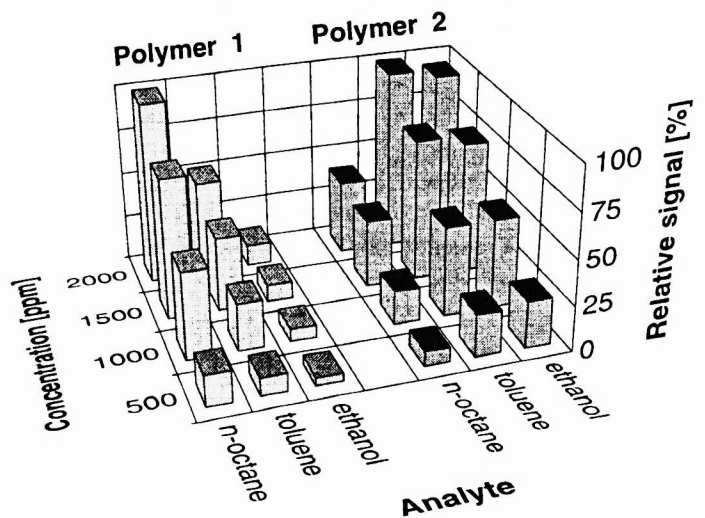


Fig. 7: Relative output signal of the capacitive chemical microsystem as a function of the analyte concentration for two different polymer coatings and three different analytes (n-octane, toluene, and ethanol); the relative signal is the ratio of the measured frequency shift to the maximum frequency shift obtained for a particular sensor/polymer combination at 2000 ppm.

The capacitive chemical microsystem is packaged using flip-chip technology [8]. This packaging approach makes it possible to expose the sensing structures to the environment while protecting the reference structures and the circuitry. The chemical sensor dice are flip-chip mounted to a ceramic substrate, which has openings for the sensing structures. The metal

frame surrounding the sensing capacitors in Fig. 6 seals the references and the circuitry from the environment after flip-chip bonding.

Upon exposure to a certain analyte concentration, the polymer absorbs analyte and changes its volume and dielectric constant. The resulting capacitance change, which is proportional to the analyte concentration, is measured with the on-chip read-out circuitry and results in a frequency shift of the output signal [8]. Fig. 7 shows the relative sensor output signal, i.e., the ratio of the measured frequency shift to the maximum frequency shift obtained for a particular polymer coating at 2000 ppm analyte concentration, as a function of the analyte concentration measured for two different polymer coatings and three different analytes (toluene, ethanol, and n-octane). The different sensitivities of the polymer coated sensor structures towards different analytes can be clearly seen. By using different polymers as sensitive layers, the selectivity of the microsystem towards specific analytes can be improved: while the sensor covered with polymer 1 is most sensitive towards n-octane, the sensor covered with polymer 2 is most sensitive towards ethanol and toluene (see Fig. 7). The detection limit of the current microsystem depends on the polymer/analyte combination and is typically of the order of 60-450 ppm [8].

Additional selectivity can be achieved by varying the thickness of the polymer coating [12]. For small polymer thicknesses (as in the case of Fig. 7), the capacitance change is dominated by the volume change of the polymer, while for large polymer thicknesses the change of the average dielectric constant of the polymer with incorporated analyte is mainly responsible for the capacitance change.

Resonant Chemical Microsensor

Gravimetric or resonant CMOS chemical microsensors can be viewed as the silicon version of the well-known quartz-crystal microbalance (QCM) used, e.g., in deposition equipment to monitor film thickness. The resonant chemical sensors investigated at PEL consist of a silicon cantilever beam coated with a chemically sensitive polymer (see Fig. 8, [9]). Absorption of analyte into the polymer increases its mass resulting in a decrease of the fundamental resonance frequency of the cantilever beam.

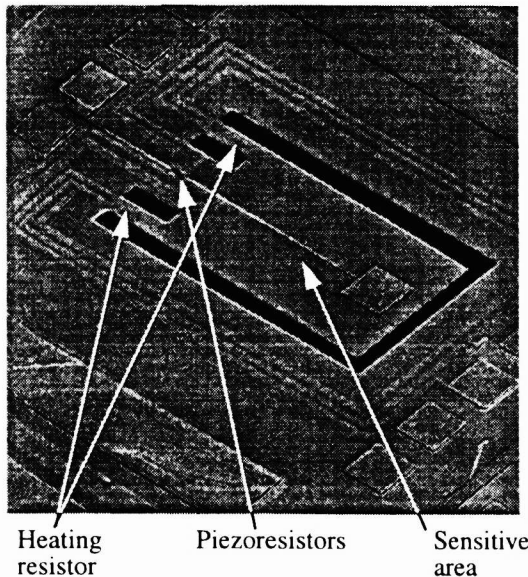


Fig. 8: CMOS cantilever beam resonator used for detection of VOCs; the 600 μm by 300 μm cantilever was fabricated using a 2 μm CMOS technology of AMS and released using a combination of bulk-micromachining from the back of the wafer with electrochemical etch-stop and RIE etching; the devices feature electrothermal excitation and piezoresistive detection of transverse vibrations [9].

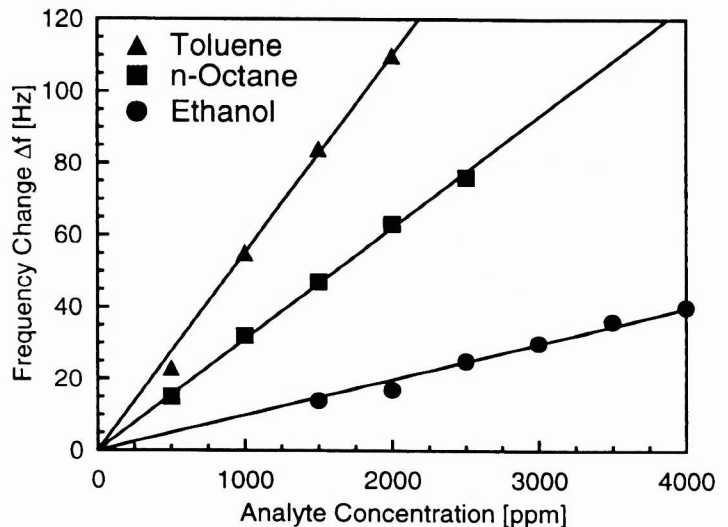


Fig. 9: Frequency shift of a 300 μm by 300 μm resonant chemical sensor covered with a 1.5 μm thick sensitive layer of polyetherurethane as a function of toluene, n-octane, and ethanol concentrations [9]; the fundamental resonance frequency of the cantilever beam is approximately 120 kHz.

The cantilever structures are released after completion of the CMOS process using a combination of anisotropic etching from the back of the wafer with an electrochemical etch-stop technique and Reactive-Ion-Etching from the wafer front. The resulting devices consist of the n-well of the CMOS process covered with the dielectric layers. Electrothermal excitation is used to excite the cantilever beams at their fundamental resonance frequency, while piezoresistive detection is employed to sense the transverse beam vibrations. The necessary resistors for excitation and detection are standard components of CMOS processes. The piezoresistors are arranged in a Wheatstone bridge and are located on the central suspension beam which is thermally isolated from the heating elements by two openings (see Fig. 8).

The lateral dimensions of the cantilever beams have been optimized with respect to the quality factor of the fundamental resonance. Q-factors in air of up to 500 have been measured for 300 μm by 300 μm silicon beam resonators with a fundamental resonance frequency of approximately 120 kHz [9]. Fig. 9 shows the frequency change of a 300 μm by 300 μm resonant chemical sensor as a function of toluene, n-octane and ethanol concentrations [9]. The silicon cantilever beam was coated with a 1.5 μm thick polyetherurethane film as sensitive layer. With the current frequency stability of the resonance frequency of 10 Hz, toluene concentrations down to 250 ppm can be resolved.

4. CMOS AFM PROBES

The last device described in this paper is a CMOS force sensor for application in Atomic Force Microscopy (AFM) allowing parallel scanning for increased throughput [13]. The nanosystem shown in Fig. 10 combines on a single chip (i) two cantilevers with piezoresistive deflection detection for parallel scanning, (ii) thermal actuators for independent deflection of the two cantilevers, and (iii) offset compensation and signal conditioning circuitry. The on-chip circuitry for the force sensor is described in detail in [14]. The integrated thermal actuators allow independent deflection of the cantilevers for parallel scanning as well as vibration excitation for dynamic mode operation of the sensors.

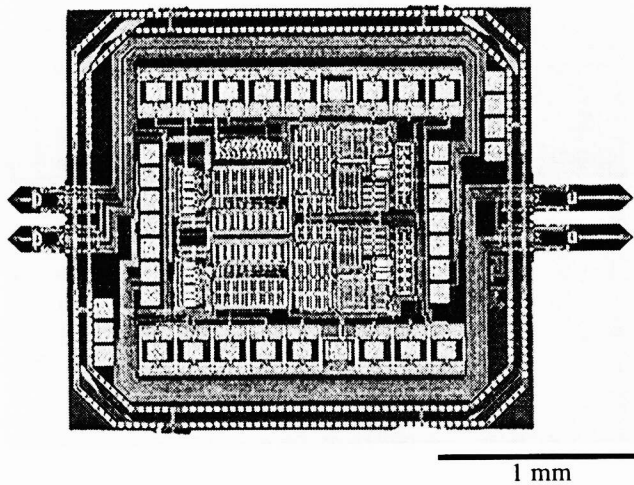


Fig. 10: Micrograph of AFM chip fabricated using a 2 μm CMOS process of AMS in combination with anisotropic etching using KOH and reactive-ion-etching; the AFM chip comprises two sets of parallel cantilevers, which are operated alternatively, and the read-out circuitry [13].

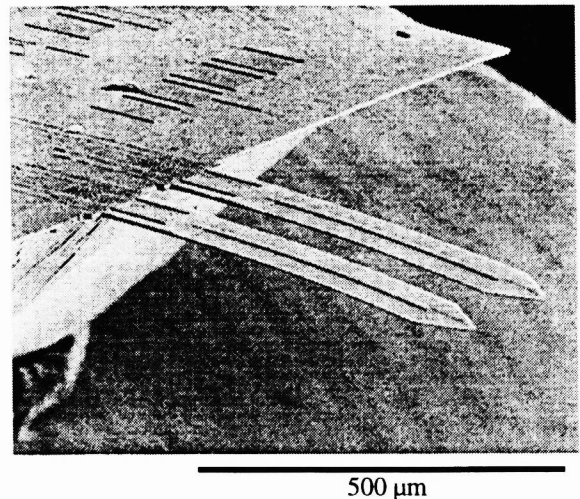


Fig. 11: SEM photograph of the released 500 μm long AFM cantilevers with integrated piezoresistors and thermal actuators [13].

The devices are fabricated using a 2 μm CMOS process of Austria Mikro Systeme International, Austria. The cantilever beams are released using anisotropic etching from the wafer back with an electrochemical etch-stop technique on CMOS n-wells in combination with two Reactive-Ion-Etching steps. After post-processing, the force sensor dice (see Fig. 10) consisting of two arrays with two cantilevers and the circuitry on an substrate island are connected to the wafer through thin support beams only. In a final processing step, the dice are pressed out of the wafer. The AFM cantilevers consist of the CMOS n-well covered by the dielectric layers. An SEM photograph of two 500 μm long cantilever beams is shown in Fig. 11. To

enhance image quality, an add-on diamond tip was mounted onto the cantilevers. The fabrication sequence of the diamond tips and a process sequence for the wafer level transfer of the tips are described in [15] and [16], respectively.

For testing, the CMOS AFM chip was mounted in a conventional AFM (Nanoscope IIIa, Digital Instruments). This makes it possible to use the Nanoscope's scanning unit and software to process the measurement data. Fig. 12 shows a parallel scanning image of a silicon grating recorded in contact mode [13]. Scanning was performed in air and no feedback was applied. Therefore, the scanning image represents the physical deflection of the cantilevers as sensed with the piezoresistors and amplified with the on-chip amplifier. The on-chip fully differential low-noise amplifier provides an amplification of 23 with a 3dB-bandwidth of 300 kHz and has a thermal noise floor of $6 \text{ nV/Hz}^{1/2}$ with a corner frequency of 10 kHz [14]. The resolution of the images taken in contact mode is better than 4 nm. While parallel imaging with two cantilevers has been demonstrated [13], the extension to fabrication of larger cantilever arrays is straight-forward in the CMOS fabrication approach.

Fig. 13 shows an image of a $1 \mu\text{m}$ grating with 15 nm line height recorded with the CMOS AFM chip in dynamic (tapping) mode [13]. In the tapping mode, the cantilever beams are excited at their fundamental resonance frequency of 20 kHz

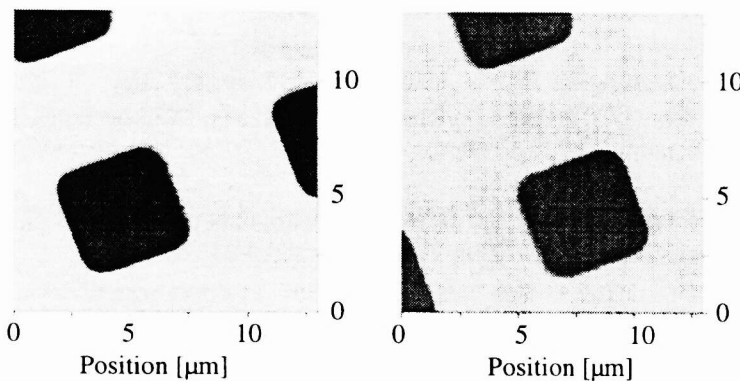


Fig. 12: Parallel scanning AFM image of silicon grating with $5 \mu\text{m}$ by $5 \mu\text{m}$ pits recorded in contact mode; the depth of the pits is 180 nm [13].

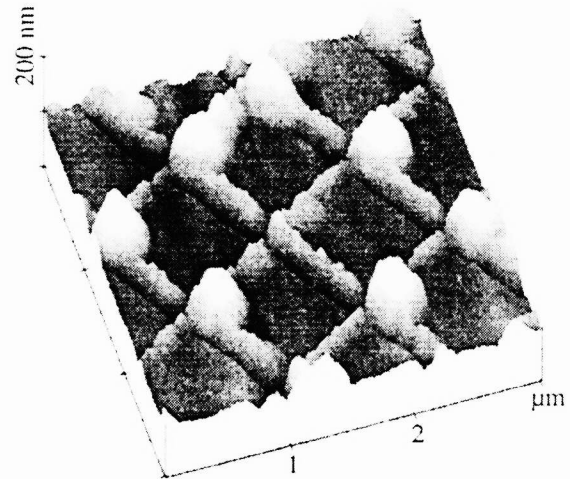


Fig. 13: Dynamic mode image of a $1 \mu\text{m}$ grating with 15 nm line height taken with the CMOS AFM chip [13].

with the integrated heating resistors by applying an ac voltage superimposed on a dc voltage. Using the height adjustment capability of the Nanoscope, the AFM chip is adjusted in a way that the cantilever gets in soft contact with the sample surface at its maximum deflection. Therefore, the vibration amplitude of the cantilever beam contains the information of the sample topography. The amplitude signal is amplified and fed-back to the height adjustment piezotubes of the Nanoscope in order to maintain a constant distance between cantilever tip and scanned surface, i.e., a constant vibration amplitude. The resolution achieved in tapping mode is better than 2 nm.

5. ACKNOWLEDGMENTS

The authors are greatly indebted to current and former staff of the Physical Electronics Laboratory at ETH Zurich, notably C. Hagleitner, A. Hierlemann, S. Kawahito (on leave from Toyohashi University, Japan), A. Koll, D. Lange, U. Münch, O. Paul, A. Schaufelbühl, N. Schneeberger, and M. Wälti, from whose publications they quote in this paper.

Financial support of the Swiss federal priority program MINAST (Micro- and Nano-Systems Technology) is gratefully acknowledged.

The infrared microsystems are developed within the MINAST project CEMSYST. The authors wish to thank their project partners Q. Huang and C. Menolfi, both from the Integrated Systems Laboratory, ETH Zurich, E. Doering from EM Micro-electronic-Marin SA, and M. Loepfe from Siemens Building Technologies, Cerberus Division, for their contributions.

The CMOS AFM chip is developed within the MINAST project FAMOS (Fast Scanning Probe Microscopes On Silicon). The help of the project partners T. Akiyama and U. Staufer, both from University of Neuchâtel, A. Tonin and H. R. Hidber, both from University of Basel, P. Niedermann from CSEM SA, L. Howald from Nanosurf AG, and P. Vettiger from IBM Research Division, Zurich Research Laboratory, is gratefully acknowledged.

6. REFERENCES

1. H. Baltes, O. Paul, and O. Brand, "Micromachined thermally-based CMOS microtransducers," *Proc. IEEE*, vol. 86, pp. 1660-1678, 1998.
2. H. Baltes, O. Brand, and O. Paul, "CMOS MEMS technology and CAD: the case of thermal microtransducers," *Proc. SPIE*, vol. 3328, pp. 2-12, 1998.
3. N. Schneeberger, *CMOS Microsystems for Thermal Presence Detection*, Ph.D. thesis, ETH Zurich No. 12675, 1998.
4. N. Schneeberger, O. Paul, and H. Baltes, "Spectral infrared absorption of CMOS thin film stacks," *IEEE Int. Conf. on MEMS (MEMS '99)*, Technical Digest, IEEE, 1999, pp. 106-111.
5. P. Malcovati, *CMOS Thermoelectric Sensor Interfaces*, Ph.D. thesis, ETH Zurich No. 11424, 1996.
6. U. Münch, D. Jaeggi, K. Schneeberger, A. Schaufelbühl, O. Paul, H. Baltes, and J. Jasper, "Industrial fabrication technology for CMOS infrared sensor arrays," *Digest Tech. Papers Transducers 97*, vol. 1, Chicago, 1997, pp. 205-208.
7. A. Koll, A. Schaufelbühl, N. Schneeberger, U. Münch, O. Brand, H. Baltes, C. Menolfi, and Q. Huang, "Micromachined CMOS calorimetric chemical sensor with on-chip low noise amplifier," *IEEE Int. Conf. on MEMS (MEMS '99)*, Technical Digest, IEEE, 1999, pp. 547-551.
8. A. Koll, S. Kawahito, F. Mayer, C. Hagleitner, D. Scheiwiler, O. Brand, and H. Baltes, "A flip-chip packaged CMOS chemical microsystem for detection of volatile organic compounds," *Proc. SPIE*, vol. 3328, pp. 223-232, 1998.
9. D. Lange, A. Koll, O. Brand, and H. Baltes, "CMOS chemical microsensors based on resonant cantilever beams," *Proc. SPIE*, vol. 3328, pp. 233-243, 1998.
10. H. Baltes, D. Lange, and A. Koll, "The electronic nose in Lilliput," *IEEE Spectrum*, vol. 35, no. 9, pp. 35-38, 1998.
11. C. Menolfi and Q. Huang, "A low noise CMOS instrumentation amplifier for thermoelectric infrared detectors," *IEEE J. Solid State Circ.*, vol. 32, pp. 1-9, 1997.
12. A. Koll, A. Kummer, O. Brand, and H. Baltes, "Discrimination of volatile organic compounds using CMOS capacitive chemical microsensors with thickness adjusted polymer coating," *Proc. SPIE*, vol. 3673, 1999, this volume.
13. D. Lange, T. Akiyama, C. Hagleitner, A. Tonin, H. R. Hidber, P. Niedermann, U. Staufer, N. F. de Rooij, O. Brand, and H. Baltes, "Parallel scanning AFM with on-chip circuitry in CMOS technology," *IEEE Int. Conf. on MEMS (MEMS '99)*, Technical Digest, IEEE, 1999, pp. 447-452.
14. C. Hagleitner, D. Lange, T. Akiyama, A. Tonin, R. Vogt, and H. Baltes, "On-chip circuitry for a CMOS parallel scanning AFM," *Proc. SPIE*, vol. 3673, 1999, this volume.
15. Ph. Niedermann, W. Hänni, D. Morel, A. Perret, N. Skinner, P.-F. Indermühle, N. F. de Rooij, and P.-A. Buffat, "CVD diamond probes for nanotechnology," *Appl. Phys. A*, vol. 66, pp. 31 - 34, 1998.
16. T. Akiyama, U. Staufer, and N.F. de Rooij, "Wafer- and piece-wise Si tip transfer technologies for applications in scanning probe microscopy," *J. Micromech. Microeng.*, 1999, to be published.